Multiple Nonlinear Optical Interactions with Arbitrary Wave Vector Differences

Keren Fradkin-Kashi,* Ady Arie, Pavel Urenski, and Gil Rosenman

Department of Electrical Engineering–Physical Electronics, Faculty of Engineering, Tel-Aviv University, Tel-Aviv 69978, Israel
(Received 12 June 2001; published 26 December 2001)

We present a novel method for simultaneously phase matching several nonlinear optical interactions within a single crystal. Quasiperiodic modulation of the nonlinear coefficient enables one to achieve high frequency mixing efficiencies for interactions with arbitrary wave vector differences. Doubling of two different frequencies as well as direct frequency tripling is experimentally demonstrated. The temperature- and wavelength-dependent properties of these interactions are explored. We discover that periodic approximation to the quasiperiodic structure shifts the phase-matched wavelengths.

PACS numbers: 42.70.Mp, 42.79.Nv

Phase matching between interacting waves in a nonlinear optical interaction is an essential condition for achieving high frequency conversion efficiency. Although naturally a wave vector difference, Δk, is caused by the dispersion of the nonlinear material, it can be compensated by several methods (see Table I). Traditionally, this was achieved using the birefringence properties of the nonlinear material [1,2]. In 1962, Armstrong *et al.* [3] proposed the scheme of quasiphase matching (QPM), by applying a periodic variation to the sign of the second order nonlinear coefficient. A modulation with a period Λ can phase match interactions with a wave vector difference that equals integral multiples of $2\pi/\Lambda$ over the transparency range of the nonlinear crystal. In ferroelectric crystals QPM can be realized by electric field poling (for a review, see Ref. [6]). However, periodic modulation of the nonlinear coefficient cannot phase match simultaneously two processes, unless their wave vector differences ratio is an integral number. Therefore, it usually fails to give a solution when phase matching is required for several nonlinear interactions simultaneously. One example is third-harmonic generation (THG), which requires phase matching both for the second-harmonic generation (SHG) process ($\omega \rightarrow 2\omega$) and the sum frequency generation (SFG) process of the fundamental frequency and its second harmonic ($\omega + 2\omega \rightarrow 3\omega$). This process can be realized in a two-step cascaded process [7], but the reduced interaction length for each stage leads to lower efficiency. In addition, the cascaded process operates only in one direction of propagation (SHG must come before SFG). Other examples, where simultaneous phase matching is required, include multiple-wavelength SHG ($\omega_1 \rightarrow 2\omega_1$ and $\omega_2 \rightarrow 2\omega_2$) and frequency quadrupling ($\omega \rightarrow 4\omega$).

In order to simultaneously phase match two interactions, aperiodic modulation of the nonlinear coefficient is required. In previous works, a Fibonacci-based modulation has been used [4]. The Fibonacci-based structure consists of two incommensurate building blocks, L and S, that are superimposed according to the Fibonacci sequence [8]. Unlike the periodic case, in which one index is required for the notation of the reciprocal vectors, here two integers are required, and the reciprocal vectors are given by $k_{mn} = 2\pi(m + n\tau)/D$, where $\tau = (1 + \sqrt{5})/2$ is the golden ratio and $D = \tau L + S$ is the average lattice parameter. Therefore, this structure can provide more reciprocal vectors and consequently enables one to phase match more interactions simultaneously. However, the expression for k_{mn} implies that the wave vector differences of the interactions cannot be arbitrarily chosen because τ is a specific number. In this sense, the Fibonacci-based structures still provide a somewhat limited solution. Indeed, recently, two extensions were made to these structures [9,10], yet both of them require some specific relation between the wave vector differences of the phase-matched interactions. Therefore, in many cases the Fibonacci-based solutions may not be applicable.

In this Letter, we experimentally demonstrate a novel method for simultaneously phase matching any two

TABLE I. Phase-matching methods and the corresponding conditions on the wave vector difference.

Phase-matching method	Condition on the wave vector difference	Ref.
Birefringent phase matching	$\Delta k = 0$	[1,2]
Periodic quasiphase matching	$\Delta k = \dfrac{2\pi m}{\Lambda}$	[3]
Fibonacci-based quasiperiodic structure	$\Delta k = \dfrac{2\pi(m + n\tau)}{D}; \ \tau = \dfrac{1 + \sqrt{5}}{2}$	[4]
Generalized quasiperiodic structure	$\Delta k = \dfrac{2\pi(m + n\tau')}{D}; \ \tau' \text{ arbitrary}$	[5, this work]

arbitrarily chosen nonlinear interactions, by using a generalized quasiperiodic structure (GQPS). The order of the building blocks in the GQPS is no longer dictated by the Fibonacci series. The reciprocal vectors are given by $k_{mn} = 2\pi(m + n\tau')/D'$, where $D' = \tau'L + S$ is the average lattice parameter and τ' is an arbitrary number [5]. Hence, the GQPS's can efficiently phase match multiple nonlinear interactions with an arbitrary ratio between their wave vector differences. In addition to having efficiencies similar to cascaded processes, the GQPS-based mixers have the same efficiency in both directions of light propagation.

Two GQPS's were designed: one for generating the second harmonic of two frequencies (1510 → 755 nm and 1064.4 → 532.2 nm), and the other for directly generating the third harmonic (1544 → 514.7 nm) via simultaneous SHG and SFG processes. The desired multiple interactions determine the wave vector differences that need to be compensated by the GQPS, and these set the order of appearance of the two building blocks as well as the average lattice parameter [5]. Three degrees of freedom remain to be determined via an optimization process: L and the duty cycles of L and S, d_L and d_S, respectively. The duty cycle is defined as the ratio of the upward subdomain to the whole block. For the optimization process, we use the Fourier transform relation between the nonlinear coefficient function, $d(z)$, and the conversion efficiency function [11,12]. Let us define a normalized structure function, $g(z) = d(z)/d_{ij}$ (where d_{ij} is the nonlinear coefficient tensor element used in the specific interaction), and denote its Fourier transform as a function of the wave vector difference as $G(\Delta k)$. Assuming negligible pump depletion and weak focusing, the conversion efficiency is proportional to $|G(\Delta k)|^2 = [d_{\mathrm{eff}}(\Delta k)/d_{ij}]^2 l^2$, where l is the crystal length. Therefore, the effective nonlinear coefficient is given by $d_{\mathrm{eff}}(\Delta k) = d_{ij}|G(\Delta k)|/l$, where the Fourier transform of the GQPS is

$$
\begin{aligned}
G(\Delta k) = \sum_{\{z_L\}} \exp(jz_L\Delta k) \cdot \Bigg[& d_L L\, \mathrm{sinc}\!\left(\frac{d_L L\Delta k}{2}\right)\exp\!\left(-j\,\frac{d_L L\Delta k}{2}\right) \\
& - (1 - d_L)L\, \mathrm{sinc}\!\left(\frac{(1 - d_L)L\Delta k}{2}\right)\exp\!\left(j\,\frac{(1 - d_L)L\Delta k}{2}\right) \Bigg] + \sum_{\{z_S\}} \exp(jz_S\Delta k) \\
\times \Bigg[& d_S(D' - \tau'L)\, \mathrm{sinc}\!\left(\frac{d_S(D' - \tau'L)\Delta k}{2}\right)\exp\!\left(-j\,\frac{d_S(D' - \tau'L)\Delta k}{2}\right) - (1 - d_S)(D' - \tau'L) \\
& \times \mathrm{sinc}\!\left(\frac{(1 - d_S)(D' - \tau'L)\Delta k}{2}\right)\exp\!\left(j\,\frac{(1 - d_S)(D' - \tau'L)\Delta k}{2}\right) \Bigg]. \qquad (1)
\end{aligned}
$$

The goal of the optimization is to find the values of L, d_L, and d_S that maximize d_{eff} for the desired interactions, and this was achieved by searching numerically over discrete lists of values. The range of possible values for the duty cycles was between 0.05 and 0.95 (with 0.05 jumps) and L varied between 4 and 12 μm (with 1 μm jumps). In addition, we required that no subdomains be smaller than 2 μm, which is currently the resolution limit of the electric field poling technique in KTiOPO$_4$ (KTP). According to the results of this optimization we designed the GQPS's for this experiment. For the dual-wavelength SHG, the parameters of the GQPS are $L = 8$ μm (hence $S = 10.6$ μm), $d_L = 0.7$, $d_S = 0.2$, and the order of the first 13 elements is LSLLSLSLLSLSL .... For the frequency tripler, the parameters are $L = 8.5$ μm (hence $S = 9.5$ μm), $d_L = 0.35$, $d_S = 0.75$, and the order is LSLLSLLSLLSLS .... The total length of each GQPS is ~10 mm, and both of them were fabricated side by side on the same KTP crystal by the low-temperature electric field poling technique [13].

The optical performance of the GQPS's was characterized using three different lasers: a Nd:YAG laser at 1064.4 nm and two tunable diode lasers near 1.55 μm and 780 nm. All lasers lased in a continuous-wave single longitudinal and spatial (TEM$_{00}$) mode and were linearly polarized in the extraordinary direction of the crystal. The mixing processes occur through the largest nonlinear coefficient in KTP, $d_{33} = 14.9$ pm/V. With the GQPS designed for multiple-peak SHG, we measured maximal normalized internal conversion efficiencies of 25%/(W · cm) and 0.073%/(W · cm) for the SHG of 1064.4 and 1509.9 nm, at crystal temperatures of 34 °C and 25 °C, respectively (Fresnel reflections were taken into account). The measured SHG powers as a function of the crystal temperature are shown in Fig. 1. Note that the ratio between the wave vector differences for these two interactions, ~2.58, cannot be provided either by a periodic modulation or by the Fibonacci-based modulation of the nonlinear coefficient.

The Nd:YAG laser at 1064.4 nm and the external cavity laser at 1509.9 nm had power levels of 123 mW and 4.78 mW, respectively. Both of the laser beams had slightly elliptic profiles with average beam radii of ~20 μm, which is close to the optimal value [14]. Our numerical simulations predict effective nonlinear coefficients of $0.293d_{33}$ and $0.322d_{33}$ for the frequency doubling processes of 1064.4 and 1509.9 nm, respectively, in this GQPS. Taking into account Miller's delta, the theoretical internal efficiencies should be 0.28%/(W · cm) and 0.103%/(W · cm), respectively [14]. Considering the ellipticity of the beams and possible imperfections of the
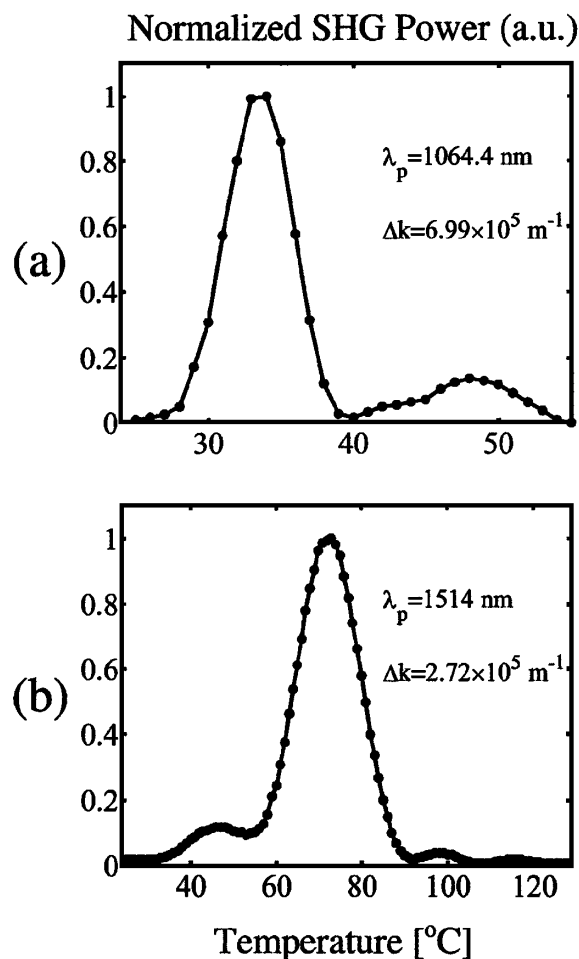
Normalized SHG Power (a.u.)

FIG. 1.   Normalized SHG powers as a function of crystal temperature measured with a GQPS in KTP designed for dual-wavelength SHG; (a) SHG of 1064.4 nm; (b) SHG of 1514 nm.
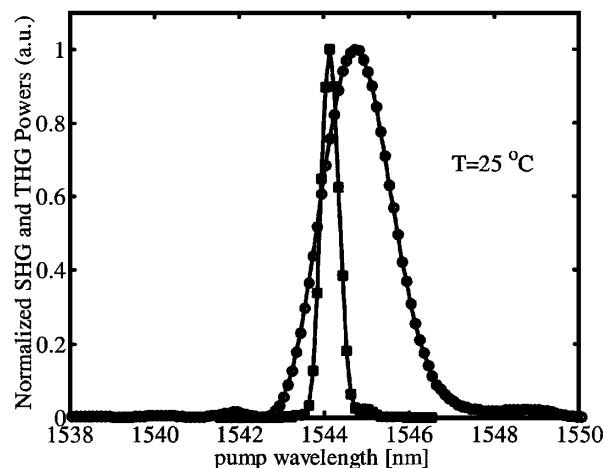

FIG. 2.   Normalized SHG (circles) and THG (squares) powers as a function of pump wavelength measured with a GQPS in KTP designed for frequency tripling.

quasiperiodically poled crystal, the measured efficiencies are in good agreement with the theoretically calculated efficiencies.

With the GQPS designed for frequency tripling, we measured separate efficiencies of 0.049%/(W · cm) and 2.15%/(W · cm) for the SHG and SFG processes, respectively. The ratio between the wave vector differences for the SHG and SFG interactions, ~2.74, could not be provided either by a periodic or by the Fibonacci-based modulation. The measured SHG power as a function of the fundamental wavelength is shown in Fig. 2.

For the case of SFG of the fundamental wave with its second harmonic, the focusing function becomes identical to that of SHG [14,15]. Our numerical simulations predict effective nonlinear coefficients of $0.236d_{33}$ and $0.426d_{33}$ for the SHG and SFG processes, respectively. Taking into account Miller's delta, the theoretical efficiencies should be 0.051%/(W · cm) and 2.47%/(W · cm), respectively. It can be seen that both of the measured efficiencies are in very good agreement with the theoretical ones.

In order to observe direct frequency tripling, we coupled the light from the tunable laser near 1.55 μm into a

fiber and passed it through a 30-dBm erbium-doped fiber amplifier. Because of the coupling to fibers, the focusing conditions in the THG measurements were slightly different than those in the SHG and SFG measurements. With ~1 W of laser power at 1544.14 nm incident on the crystal at room temperature, and a beam radius of ~30 μm in the middle of the crystal, a maximum THG power of 50.5 nW is measured. This indicates a THG efficiency of 3×10^{-5}%/(W^2 · cm^2). The measured THG power as a function of the fundamental wavelength is shown in Fig. 2. The THG efficiency for a crystal with length l is given by $\eta_{THG} = P_{3\omega}/(P_\omega^3 l^2) = (\eta_{SHG} \eta_{SFG})/2$. Based on the measured SHG and SFG efficiencies, we estimate an upper limit for the expected THG efficiency. At the peak wavelength of the THG process (1544.14 nm) we measure a SHG efficiency, which is only ~75% of the maximal SHG efficiency, and a SFG efficiency, which is only ~80% of the maximal SFG efficiency. Based on these, we estimate an upper limit to the THG efficiency of 3.2×10^{-4}%/(W^2 · cm^2). The discrepancy is mostly due to the change in the focusing conditions, which has slightly shifted the phase-matching points for the SHG and SFG, as well as decreased the maximal efficiency due to nonoptimal focusing conditions.

We designed and fabricated another GQPS in KTP in order to investigate the effects of a periodic approximation to the quasiperiodic sequence. To implement the periodic approximation we created a basic set, which consisted of the first 13 building blocks of the GQPS used for frequency tripling. The basic set was repeated throughout the entire length of the KTP crystal. When we repeated our measurements with this GQPS, we discovered, for the first time to the best of our knowledge, that the periodic approximation shifted the SHG and SFG phase-matching points in opposite directions. As a result, we were able to obtain simultaneous SHG and SFG, but not direct THG. We numerically calculated the expected effect of this partitioning on the phase-matching point. We found out that as the length of
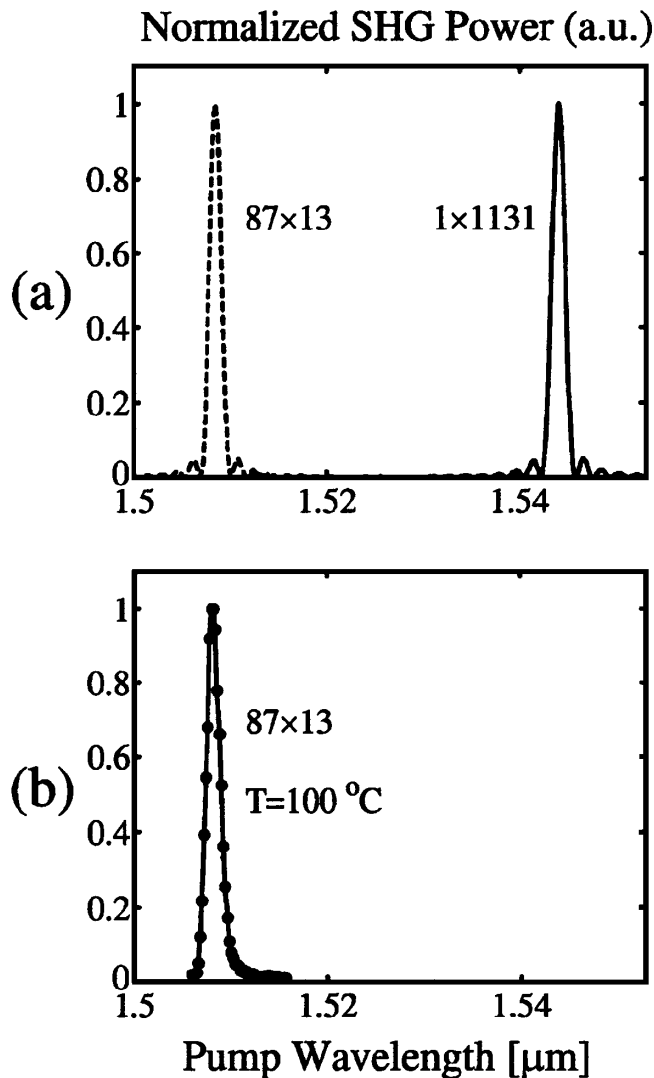
FIG. 3. Normalized SHG power as a function of pump wavelength measured with a GQPS in KTP; (a) calculated without partitioning (1 × 1131, solid line) and with partitioning (87 × 13, dashed line); (b) measured with partitioning (87 × 13).

the constructing sets becomes shorter, the phase-matched wave vectors are shifted more significantly, and the ratio between them changes. For example, with partitioning into 13-element sets, the ratio between the wave vector differences for the SHG and SFG interactions is 2.56, which is 6.5% smaller than the designed ratio, 2.74. Figure 3 shows the shift of the phase-matching point for the SHG process, and it can be seen that the numerical calculation based on our theoretical model predicts this shift and fits the experimental results.

In conclusion, we have designed and fabricated a novel one-dimensional GQPS for nonlinear optics applications and explored its temperature- and wavelength-dependent properties. This novel structure has the ability to simultaneously phase match completely arbitrarily chosen interactions, whose wave vector differences are, by no means, related to each other. This represents a significant extension in the design flexibility with respect to the existing structures, i.e., periodic and Fibonacci-based structures. In addition to single-pass frequency up-conversion processes, which are demonstrated in this Letter, many nonlinear processes require simultaneous phase matching and numerous new optical devices may be realized. For example, a quasiperiodic frequency mixer, which is suitable both for phase matching of an optical parametric oscillator, as well as for sum-frequency generation of the pump and signal (or idler), can provide tunable radiation at wavelengths shorter than the pump wavelength. We have studied both numerically and experimentally the effects of a periodic approximation to the GQPS and have found out that such approximation shifts the phase-matching points in the wave vector mismatch domain.

The GQPS's proposed here are relevant to many fields in fundamental physics other than nonlinear frequency conversion. The ability to simultaneously phase match two processes can be used for adiabatic shaping of quadratic solitons [16] owing to the ability of solitons to adapt themselves adiabatically to the local wave vector mismatch that they experience. Whereas our GQPS's were implemented in a ferroelectric material, they may be realized in many other different materials such as semiconductor heterostructures [17], dielectric thin films [18], ferromagnetic materials [19], etc., and can be explored by a variety of physical effects, such as x-ray and Raman scattering [17], ultrasonic interactions [20], etc.

*Email address: kerenfr@post.tau.ac.il

[1] J. A. Giordmaine, Phys. Rev. Lett. **8**, 19 (1962).
[2] P. D. Maker *et al.,* Phys. Rev. Lett. **8**, 21 (1962).
[3] J. A. Armstrong *et al.,* Phys. Rev. **127**, 1918 (1962).
[4] S.-N. Zhu, Y.-Y. Zhu, and N.-B. Ming, Science **278**, 843 (1997).
[5] K. Fradkin-Kashi and A. Arie, IEEE J. Quantum Electron. **35**, 1649 (1999).
[6] R. L. Byer, J. Nonlinear Opt. Phys. **6**, 549 (1997).
[7] K. Kintaka *et al.,* Electron. Lett. **33**, 1459 (1997).
[8] D. Levine and P. J. Steinhardt, Phys. Rev. B **34**, 596 (1986).
[9] Y.-Q. Qin *et al.,* Appl. Phys. Lett. **75**, 448 (1999).
[10] Y.-B. Chen *et al.,* J. Phys. Condens. Matter **12**, 529 (2000).
[11] M. Nazarathy and D. W. Dolfi, Opt. Lett. **12**, 823 (1987).
[12] M. M. Fejer *et al.,* IEEE J. Quantum Electron. **28**, 2631 (1992).
[13] G. Rosenman *et al.,* Appl. Phys. Lett. **73**, 3650 (1998).
[14] G. D. Boyd and D. A. Kleinman, J. Appl. Phys. **39**, 3597 (1968).
[15] S. Guha and J. Falk, J. Appl. Phys. **51**, 50 (1980).
[16] L. Torner *et al.,* Opt. Lett. **23**, 903 (1998).
[17] R. Merlin *et al.,* Phys. Rev. Lett. **55**, 1768 (1985).
[18] E. Macia, Appl. Phys. Lett. **73**, 3330 (1998).
[19] R. Lifshitz, Phys. Rev. Lett. **80**, 2717 (1998).
[20] Y.-Y. Zhu *et al.,* Phys. Rev. B **40**, 8536 (1989).